JOURNAL OF APPLIED PHYSICS **104**, 104910 (2008)

Nanometric size effect on Ge diffusion in polycrystalline Si

A. Portavoce,[1,2,a)] G. Chai,[3] L. Chow,[3] and J. Bernardini[1,2]
[1]*Aix-Marseille Université, IM2NP, Faculté des Sciences et Techniques, Campus de Saint-Jérôme, Avenue Escadrille Normandie Niemen-Case 142, F-13397 Marseille Cedex, France*
[2]*CNRS, IM2NP (UMR 6242) Faculté des Sciences et Techniques, Campus de Saint-Jérôme, Avenue Escadrille Normandie Niemen-Case 142, F-13397 Marseille Cedex, France*
[3]*Department of Physics, University of Central Florida, Orlando, Florida 32816, USA*

(Received 25 June 2008; accepted 17 September 2008; published online 20 November 2008)

The nanosize effect on Ge diffusion ($850 \leq T \leq 1000$ °C) in polycrystalline Si layers is investigated. The Ge diffusion coefficients in microcrystalline and nanocrystalline Si layers made of 30 μm and 40 nm wide grains, respectively, are measured and compared. In the microcrystalline Si layer, the Ge diffusion coefficient in micrograin boundaries is measured using a conventional analytical solution of Fick's equations corresponding to the Fisher model. In the nanocrystalline Si layer, the Ge diffusion coefficients in nanograins and in nanograin boundaries are measured via a method based on two-dimensional simulations using the Fisher model geometry. The diffusivities in nanograins and nanograin boundaries are one order of magnitude higher than in micrograins and micrograin boundaries, respectively. However, the nanosize effect appears to be different in grains and grain boundaries; despite that the activation energy for diffusion in 40 nm wide grains is at least 1 eV lower than in Si bulk. The activation energy in nanograin boundaries is about the same as in micrograin boundaries. © *2008 American Institute of Physics*. [DOI: 10.1063/1.3010297]

I. INTRODUCTION

Solid-state atomic diffusion is an important phenomenon that controls atomic redistribution and phase transformation during industrial fabrication processes. In the past, the metallurgy industries were essentially producing microstructured materials. In order to develop and /or improve the production processes, fundamental studies have been performed on atom mobility in these structures. For this matter, several analytical solutions of Fick's equation and different models for semi-infinite materials have been used. The benefit of this method is that there is no need for simulations (faster calculations). However, the use of an analytical solution implies that the experimental conditions completely fulfill the limit conditions of the model. Thus, each solution can only be used for one particular type of experiment, and many experimental conditions have no practical analytical solutions.

In the case of polycrystals, solutions corresponding to type *A*, *B*, and *C* diffusion regimes (Harrison's classification[1]) in a semi-infinite matrix use Fisher's two-dimensional (2D) model[2] assuming that (i) the grain boundary (GB) thickness δ is equal to 0.5 nm, and that the GB diffusion coefficient (D_{gb}) is larger than the diffusion coefficient in the adjacent grains (D_g), (ii) D_g is equal to the bulk diffusion coefficient (D_b), and (iii) the GBs are immobile during heat treatments. D_b is generally too small to be measured for the typical temperature range corresponding to the different diffusion regimes observed in polycrystals. Thus, it is usually extrapolated from high-temperature measurements. The first two assumptions have been effectively verified for massive well recrystallized samples,[3,4] comparing diffusion experiments performed in type *C* and type *B* regimes. The last assumption is not easily fulfilled in refractory metals[5] and in very pure metals.[6] Numerous diffusion measurements have been performed by different authors on same systems (matrix and impurity) but using samples elaborated by different methods, with micrometric grains of different sizes. These results have been shown to exhibit, in general, a dispersion of only 10%, which is in the range of the temperature measurement error. These observations suggest that (i) the diffusivity in micrometric grains is the same as the bulk diffusivity and (ii) the assumptions made in Fisher's model are acceptable in micron-size polycrystals.

Today, as the nanotechnology market is growing, the production of different types of nanostructured materials is needed, as well as innovative elaboration processes. For example, the technology developed in silicon-based microelectronics has already reached the nanometer scale. In consequence, the fundamental aspects of solid state atomic migration need to be studied at this scale. Scaling materials down to the nanometer raises several questions. (i) Is diffusion over a nanometer distance (nanodiffusion) different from microscopic diffusion? (ii) Is diffusion through a nanometric-size phase or structure (nanosize effect) different from bulk diffusion? Moreover, the questions particularly for polycrystals are the following. (iii) Is diffusion in nano-GBs faster than in classical GBs? (iv) What is the role of triple junctions (TJs)? Regarding questions (i), (iii) and (iv), several authors have developed models and theories,[3,7–11] but only few experimental works have been performed to date.[12,13] It has been shown that during the first stage of interdiffusion between two thin layers, atom migration does not follow Fick's second law.[14,15] Diffusion enhancement up to three orders of magnitude has been reported in aluminum TJs compared to diffusion in simple GBs.[16] However, not all diffusion experiments performed in nanograin polycrystals

a)Author to whom correspondence should be addressed. Electronic mail: alain.portavoce@l2mp.fr.

 © 2008 American Institute of Physics

Author complimentary copy. Redistribution subject to AIP license or copyright, see http://jap.aip.org/jap/copyright.jsp

exhibit fast diffusion.[17] Question (ii) has not really been addressed yet, and no GB diffusion experiments have been reported in nanocrystalline semiconductors.

The study of impurity diffusion in nanograin polycrystalline layers can improve our fundamental knowledge of the nanosize effect on diffusion, especially if we are able to measure both the diffusion coefficient in the grains and in GBs. This work examines the nanosize effect on Ge diffusion in nanograin polycrystalline Si (poly-Si) via finite element simulations using the software COMSOL.[18] This method can be applied to finite layers instead of being restricted to a semi-infinite matrix, as most diffusion equation solutions generally used. It allows simultaneous measurements of the diffusion coefficients in the grains and in the GBs independently of the diffusion regime (type *A*, *B*, or *C*). The Ge–Si system is ideal for investigating nanosize effect on diffusion for the following reasons. (i) Si(Ge) layers of very high purity can be produced, which allows the same order of purity for mono, micro, and nanocrystalline layers, (ii) Ge and Si are totally miscible preventing any clustering effect during diffusion, (iii) there is no electric effect between Ge atoms and Si point defects allowing for a constant diffusion coefficient in our experimental conditions, and (iv) Ge segregation has not been observed in Si GBs.

II. EXPERIMENTS

A. Ge diffusion in microcrystalline Si

Several steps were required to prepare the samples before the diffusion experiments were performed. Boron-doped cast silicon generally used as base material for the growth of Czochralski (or floating-zone) single crystals, with a resistivity of ~0.15 Ω cm, was used as starting material. The samples were cut into slices of about $20 \times 12 \times 2$ mm^3 using a diamond saw, then cleaned in a CP6 solution [made of 1 vol. of HNO_3 (100%), 1 vol. of CH_3COOH (100%) and 1 vol. of diluted HF (50%)], and then their surfaces were mechanically and chemically polished. In a following step, the samples were annealed at 1200 °C for 2 days in quartz tubes under pure argon atmosphere, in order to promote their crystallization and to stabilize the size of the Si grains in the samples. The average grain size in the samples was estimated to be about 30 μm, and the dislocation density determined by etch pit counts was found to be about 10^7 cm^{-2}. Then, each sample was once more annealed at the same temperature as that of the following diffusion experiment. Immediately after annealing, ^{68}Ge with a specific activity of about 2 mCi /mg was chemically plated from an acidified hydrofluoric solution onto the specimen surface. Diffusion of the ^{68}Ge radiotracer was performed in quartz tubes under a pure argon atmosphere in a preheated furnace and was abruptly stopped at the end of the annealing time by cooling down the quartz tubes with water. The diffusion experiments were performed at four different temperatures: 890, 945, 999, and 1053 °C. After the diffusion treatment, the side edges and the back surface of the samples were ground off by several diffusion lengths to minimize the effect of possible side or back diffusion on radioactive counting. Penetration profiles were obtained by a mechanical sectioning technique. After each sectioning, the radiotracer activity was measured by counting the activity of the removed layer with a low temperature γ Ge–Li detector.

B. Ge diffusion in nanocrystalline Si

The sample was made of a 500 nm thick polycrystalline Si layer deposited by chemical vapor deposition (CVD) at low temperature on a B-doped Si(001) substrate of nominal resistivity 10–20 Ω cm. The use of CVD industrial reactors promotes the production of high purity samples. After deposition, Ge ions were implanted at room temperature in the polycrystalline Si layer with an energy of 180 keV and a dose of 4.2×10^{14} at cm^{-2}. The sample was then cut into several pieces; some were kept as references and others were annealed under constant ultrapure (99.999%) Ar gas flow at six different temperatures: 700, 800, 850, 900, 950, and 1000 °C. The depth profiles of Ge concentration in the samples were measured by secondary ion mass spectroscopy (SIMS). We used a CAMECA IMS-3f system operated at 10 kV with an O_2^+ primary ion beam having an impact angle of 40° compared to the normal of the sample surface. The Ge concentration profiles were measured both in the poly-Si layer and in the Si substrate in order to observe Ge diffusion in the two Si matrices. The average size of the Si grains in the polycrystalline layer was measured by x-ray diffraction (XRD) both before and after the thermal treatments. The grains were found to have the same size ~40 ± 2 nm in all the samples, which implied no grain growth during annealing. Furthermore, XRD showed that the nanograins were fully relaxed, so stress is not expected to influence the Ge diffusion in these samples.

III. RESULTS

A. Ge diffusion in microcrystalline Si

The Ge penetration profiles measured after the diffusion experiments performed at 890, 945, 999, and 1053 °C are presented in Fig. 1. Two regions must be distinguished in these profiles, as generally observed in the so-called *B* kinetic regime of diffusion. However, the logarithm of the specific activity versus the depth to the 6/5th power is linear for distances greater than $5 \times (D_g t)^{1/2}$ [i.e., 50 to $100 \times (D_g t)^{1/2}$]. In the absence of nonlinear solute segregation, the possible explanation of this extended curvature is the presence of a fraction of moving GBs during diffusion.[5] Accordingly, the profiles were analyzed using the relation

$$ln\ C = ln(q_1\ exp(-q_2 x^{6/5}) + q_3\ exp(-q_4 x)). \quad (1)$$

In this equation,[5] the first term refers to the deep-penetrating region of the profiles with a smaller slope and a lower level of tracer concentration caused by diffusion along stationary GBs, while the second term corresponds to the near-surface region of the profiles with a larger slope and a high level of tracer concentration due to moving GBs. The coefficient q_2 is equal to the slope *a* of the deeper part of the profiles presented in Fig. 1, which allows the product $P = \delta D_{gb}$ in stationary GBs to be calculated using the equation

Author complimentary copy. Redistribution subject to AIP license or copyright, see http://jap.aip.org/jap/copyright.jsp

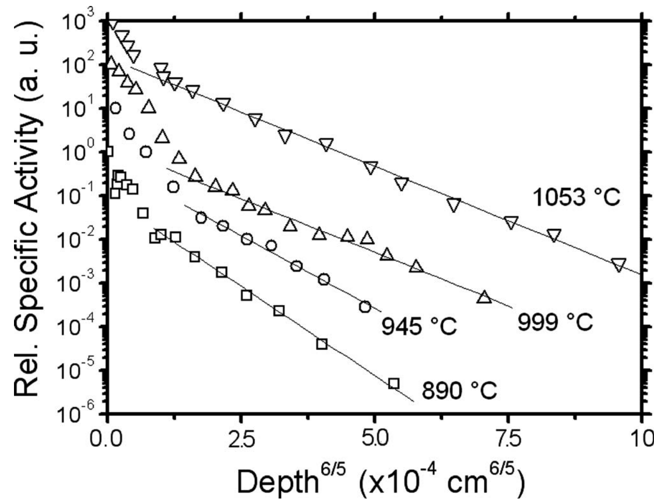

FIG. 1. The normalized concentration (arbitrary units) of the Ge radiotracer vs the depth$^{6/5}$(cm$^{6/5}$) measured in the samples after annealing at 890 °C for 11 989 920 s (□), 940 °C for 3 510 900 s (○), 999 °C for 857 640 s (△), and at 1053 °C for 2 732 040 s (▽). The slope of the linear part of the profiles (solid lines) was used to determine the diffusion coefficients at the different temperatures.

$$P = \delta D_{gb} = 1.308\left(\frac{D_g}{t}\right)^{1/2}(-a)^{-5/3} \quad \text{with } a = \frac{d \ln C}{dx^{6/5}}. \tag{2}$$

It is worth mentioning that when the profiles can be obtained far from the surface by using very sensitive detectors, this analysis leads to P values equal to those calculated using the classical Suzuoka equation.[17,19]

B. Ge diffusion in nanocrystalline Si

Figure 2 presents Ge SIMS profiles measured in the as-implanted sample (●) as well as in the samples annealed at 700 °C (○) and 800 °C (□) for 0.5 h. The profiles obtained after annealing do not exhibit any Ge diffusion compared to the profile in the as-implanted sample. Thus, the transient enhance diffusion (TED) phenomenon due to nonequilibrium defects created during implantation can be neglected in our experiments. Usually, TED can be noticed in mono-Si for temperatures lower than 700 °C and for annealing times of few minutes.[20]

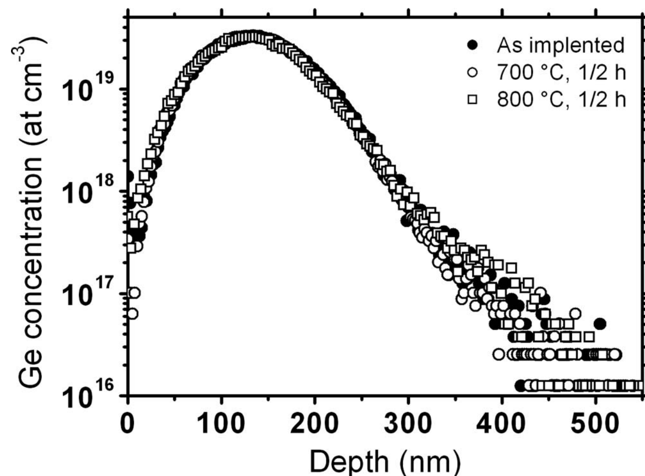

FIG. 2. Ge concentration (at cm^{-3}) vs depth (nm) measured by SIMS after implantation without annealing (●), after annealing at 700 °C (○), and 800 °C (□) for 0.5 h.

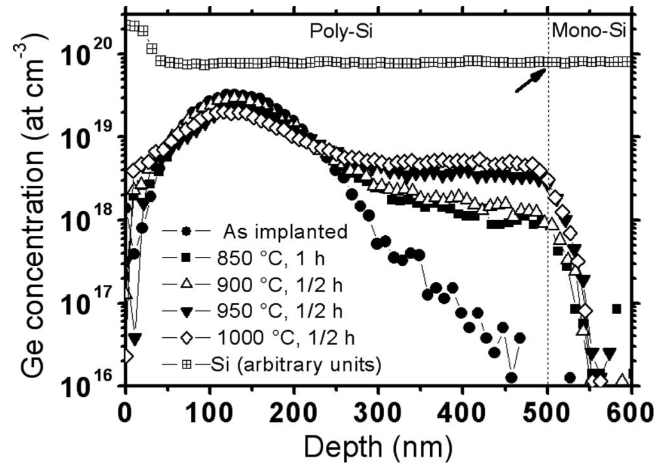

FIG. 3. Ge concentration (at cm^{-3}) vs depth (nm) measured by SIMS after implantation without annealing (●), after annealing at 850 °C for 1 h (■), and at 900 °C (△), 950 °C (▼) and 1000 °C (◇) for 0.5 h. The Si concentration profile (arbitrary units) measured after annealing at 950 °C for 0.5 h is also presented (⊞). The arrow indicates the interface between the polycrystalline Si layer and the monocrystalline Si(001) substrate.

In Fig. 3, the Ge SIMS profile obtained in the as-implanted sample (●) is compared to those measured after annealing at 850 °C for 1 h (■), and at 900 °C (△), 950 °C (▼) and 1000 °C for 0.5 h (◇). For all these thermal treatments Ge has diffused in the poly-Si layer, but Ge diffusion in the mono-Si substrate is not observed. The interface between the poly-Si layer and the Si substrate is represented by the dotted line. The slope of the SIMS profiles after this line is about the same, approximately 9 nm /decade (logarithmic scale) in all the annealed samples. It is well known that SIMS analyses induce artifacts in the concentration profiles. One of these artifacts, which is due to the displacement of the target atoms by the primary ions, consists of a slope in addition to the real one when the concentration profile decreases.[21] This artificial slope can be calculated[21] and was found to be equal to 9.5 nm /decade for our SIMS analysis conditions, which is in agreement with the 9 nm /decade slope observed experimentally. This confirms that the Ge diffusion in the mono-Si substrate is negligible. The Si concentration profiles measured by SIMS do not exhibit any singularity at the poly-Si /mono-Si interface (see arrow on Fig. 3), showing that no diffusion barrier is present at the interface (no SiO_2). In our annealing conditions, the Ge diffusion coefficient in the mono-Si matrix is too low to allow diffusion into the substrate (in agreement with the literature[22–24]). The evolution of the first region of the concentration profile (Gaussian shape) with temperature is typically due to Ge diffusion in the grains, the second region being the diffusion in GBs signature.[4] Obviously, Ge has diffused in the grains during the thermal treatments, especially at 1000 °C where the top of the Gaussian part of the profile decreases from $\sim 3\times 10^{19}$ to $\sim 2\times 10^{19}$ at cm^{-3}. This shows that the diffusion coefficient in the nanograins of the poly-Si layer is actually higher than that in the mono-Si substrate. One can also notice in Fig. 3 that no Ge segregation is observed at the

Author complimentary copy. Redistribution subject to AIP license or copyright, see http://jap.aip.org/jap/copyright.jsp

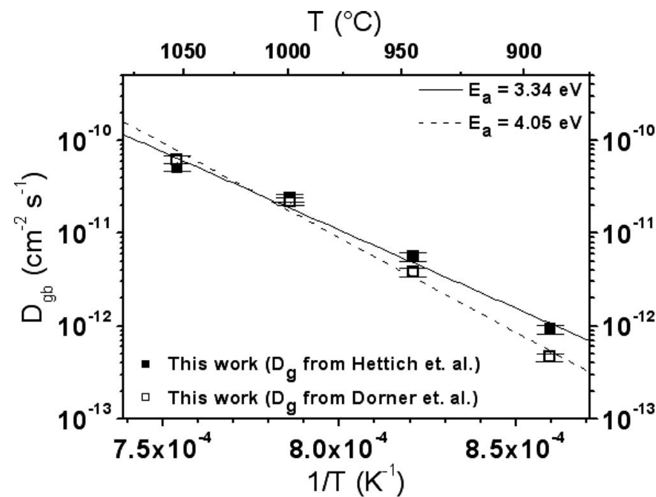

FIG. 4. Ge diffusion coefficients vs 1/T (K^{-1}) measured in the Si micro-GBs using an analytical solution of the Fisher model. Two sets of coefficients are presented: one set corresponds to the GB diffusion coefficients found using the Ge diffusion coefficient in Si bulk from Hettich *et al.* (Ref. 23) (■), and the second corresponds to the GB diffusion coefficients found using the Ge diffusion coefficient in Si bulk from Dorner *et al.* (Ref. 22) (□).

interface poly-Si /Si substrate despite the thermal treatments, showing that Ge does not segregate in Si GBs.

IV. DIFFUSION COEFFICIENT MEASUREMENTS

A. Ge diffusion in microcrystalline Si

The knowledge of the Ge diffusion coefficient in Si bulk (i.e., in-grain diffusion) is required in order to determine the product P from the slope of the experimental profiles using Eq. (2). Different results have been previously published. The measurements of McVay and Ducharme[25] were performed in polycrystalline Si and despite the fact that the authors claim that they did not notice any effect of boundary diffusion in their measurements, they found an activation energy too low to correspond to monocrystalline bulk Si diffusion. Zangenberg *et al.*[24] discussed this point in their paper; they suspect that the coefficient measured by McVay and Ducharme[25] is actually the effective diffusivity resulting from both lattice and grain boundary diffusion (type A regime). Using the SIMS technique, Zangenberg *et al.*[24] found Ge diffusion coefficients in Si bulk comparable to those measured by Hettich *et al.*[23] using radiotracers. They obtained an activation energy of ~4.65 eV, which is between the values obtained by Hettich *et al.*[23] (~3.93 eV) and Dorner *et al.*[22] (~5.34 eV), who also used the SIMS technique. However, the temperature range used by Zangenberg *et al.*[24] (900–1050 °C) is narrower than the one used by Dorner *et al.*[22] and Hettich *et al.*[23] (850–1300 °C). For these reasons, we decided to use the data from both Dorner *et al.*[22] and Hettich *et al.*[23] in order to extract the Ge diffusion coefficients in Si micro-GBs. The Ge diffusion coefficients measured in the Si micro-GBs are presented in Fig. 4. We found $D_{gb}^{Ge} = 31.65 \times 10^2 \exp(-3.34\ \text{eV}/kT)\text{cm}^2\ \text{s}^{-1}$ using the bulk diffusion coefficient from Hettich *et al.*[23] and $D_{gb}^{Ge} = 19.10 \times 10^4 \exp(-4.05\ \text{eV}/kT)\text{cm}^2\ \text{s}^{-1}$ using the bulk diffusion coefficient from Dorner *et al.*[22] The lateral size δ of GBs was chosen to be equal to 0.5 nm, as usual.[4]

B. Ge diffusion in nanocrystalline Si

The Ge diffusion coefficients have been measured using the SIMS profiles presented in Fig. 3. The method we employed consists of using the SIMS profile measured in the as-implanted sample as the initial Ge distribution, and then adjusting the diffusion coefficients in a simulation matching the experimental conditions in order to fit the SIMS profile measured after annealing. Assuming two possible diffusion paths in the samples (lattice diffusion in grains and GB diffusion), 2D simulations are needed. We decided to use the Fisher model geometry for two reasons: (i) the relevance of this model has been already demonstrated and (ii) we needed to compare our results with those obtained in microcrystalline layers that have been obtained using Fisher's model (classical approach).

In the Fisher geometry, the matrix in which the solute is diffusing is made of a GB having a length X and a width δ located between two rectangular grains of same length having a lateral size L^{1-2}. For simulation purposes, considering the symmetries of the Fisher geometry and using the proper boundary settings, the matrix structure can be simplified to a grain with a lateral size of $\frac{1}{2}L$ in contact with a GB having a width of $\frac{1}{2}\delta$. For our simulations, we used a 2D matrix having a size along the x-axis equal to the thickness X of the polycrystalline layer, and a total size along the y-axis equal to $\frac{1}{2}(L+\delta)$. Only one-dimensional (1D) concentration-versus-depth profiles are experimentally accessible via SIMS measurements. After ion implantation, the distribution of implanted Ge atoms in the grains and in the GBs was assumed to be identical. Consequently, whatever the coordinate on the y-axis of the 2D matrix (in the grain or in the GB), the initial Ge distribution along the x-axis (thickness of the layer) is identical and corresponds to the experimental as-implanted SIMS profile shown in Fig. 3. Considering this initial Ge distribution, we used the software COMSOL to solve via the finite element method the classical equation of diffusion

$$\frac{dC}{dt} = \nabla(-D\,\nabla\,C) \tag{3}$$

with C the concentration and D the diffusion coefficient of the solute in the two dimensions (x,y) of the 2D matrix. TED was neglected in the simulation, as well as the Ge diffusion in the mono-Si substrate ($X \geq 500$ nm), and we considered that Ge did not segregate in GBs. The simulation was thus dependent upon six parameters: the grain size (L), the GB width (δ), the annealing temperature (T), the annealing time (t), D_g and D_{gb}. The parameters L and δ were set to 40 and 0.5 nm,[4] respectively, T and t were chosen to match each thermal treatment. In this type of simulation, knowledge of the kinetic regime of diffusion is not necessary as the diffusion is taken fully into account in the two dimensions of the model.

The final 2D Ge distribution calculated for a given heat treatment cannot be directly compared to the 1D SIMS profile measured in the sample after annealing. The calculated 2D distribution has to be transformed into a 1D distribution, in the same way as SIMS measurements give a 1D concentration profile versus depth, while the distribution in the

Author complimentary copy. Redistribution subject to AIP license or copyright, see http://jap.aip.org/jap/copyright.jsp

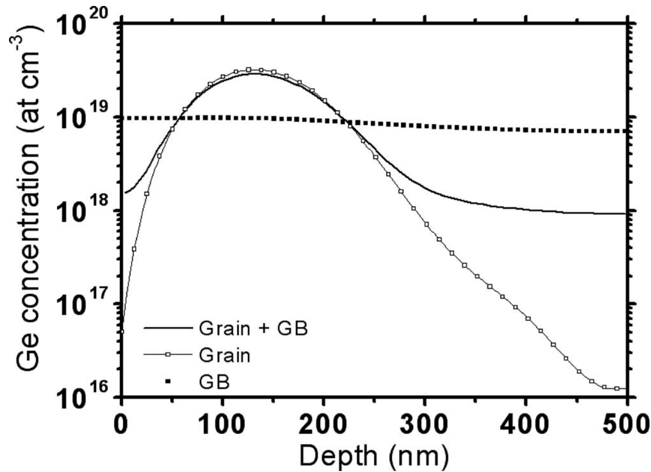

FIG. 5. 1D Ge concentration profiles resulting from the simulation of a thermal annealing at 850 °C for 1 h with $D_g=1.5\times10^{-17}$ cm^2 s^{-1} and $D_{gb}=2.5\times10^{-12}$ cm^2 s^{-1}. The average profile of Ge along the depth direction (x-axis) calculated on the whole 2D matrix is presented (solid line) with the Ge profiles in the middle of the grain ($y=0$, solid line and open squares) and in the middle of the GB ($y=20.25$ nm, solid squares).

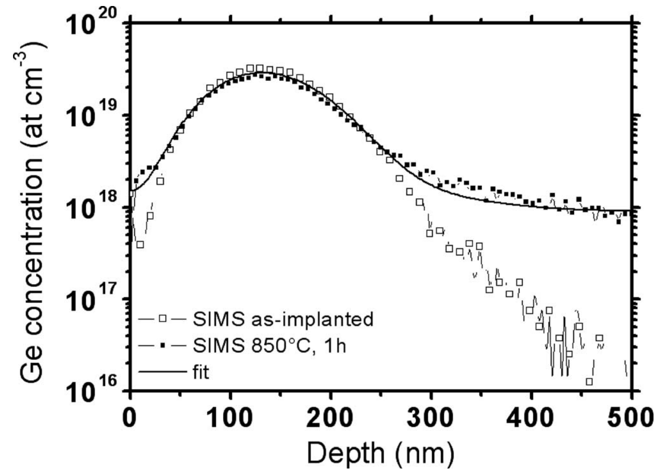

FIG. 6. Ge concentration (at cm^{-3}) vs depth (nm) measured by SIMS after implantation without annealing (□) and after annealing at 850 °C for 1 h (■), presented with the 1D profile resulting from the 2D simulation of annealing at 850 °C for 1 h with $D_g=1.5\times10^{-17}$ cm^2 s^{-1} and $D_{gb}=2.5\times10^{-12}$ cm^2 s^{-1} (solid line).

sample may be three-dimensional (3D). In our case, the surface area analyzed by SIMS is about 60×60 μm^2, while the average lateral size of the grains is about 40 nm. Thus, for a given depth (x-axis) the concentration in a SIMS profile corresponds to the average concentration of Ge atoms between zones of different concentrations pondered by their respective atomic site densities (in grains and GBs). In the same way, the 2D distribution in the simulation matrix can be transformed into a 1D concentration profile by calculating for every point along the x-axis the total average Ge concentration between areas of different concentrations (along the y-axis) pondered by their sizes. Figure 5 presents, in the case of annealing at 850 °C for 1 h with $D_g=1.5\times10^{-17}$ cm^2 s^{-1} and $D_{gb}=2.5\times10^{-12}$ cm^2 s^{-1}, the 1D Ge distributions in the middle of the grain and in the middle of the GB, with the 1D average profile calculated on the entire 2D matrix, which is comparable to SIMS measurements. The final 1D distribution is highly dependent upon the GB density (i.e., on the grain lateral size compared to δ). The bigger the grains are, the closer the total average profile and the in-grain profile are since the influence of the in-GB distribution becomes negligible in the total average of concentrations.

Following the procedure described above, D_g and D_{gb} were adjusted in order to fit the experimental SIMS profile obtained after annealing. We noticed that the shape of the left part of the diffusion profile is independent of D_{gb}. The evolution of the Gaussian part of the profile describes mainly the in-grain diffusion. In the same way, the slope of the linear part of the profile (on the right) is mainly driven by in-GB diffusion. Changing D_g does not change this slope, but changes the total amount of Ge atoms in the GBs. Because the influence of D_g and D_{gb} is different on the diffusion profile, only a single D_g-D_{gb} pair can fit each profile, allowing these two coefficients to be measured for every single profile.

Figure 6 presents the best fit of the SIMS profile that was obtained for the sample annealed at 850 °C for 1 h. The simulated profile corresponds to the average 1D distribution presented in Fig. 5. Beside the possible deviations from the real distribution of the SIMS profile due to the intrinsic inaccuracy of the technique, one of the main problems of perfectly fitting the SIMS profiles comes from the difference in total Ge dose between the as-implanted SIMS profile and the profiles obtained after annealing. Indeed, the mass is conserved during the simulation and therefore the total Ge dose in the simulated profiles is always equal to the initial dose measured in the as-implanted sample (initial Ge distribution). However the dose in the SIMS profiles measured after annealing can vary due to experimental issues. The profile measured after annealing at 850 °C during 1 h, presented in Fig. 6, is the profile having the highest dose error among our set of SIMS analyzes. It is about ~6%, while the dose error of the other profiles is only between 0.5 and 2%. Typically, the higher the dose error is, the more difficult it is to fit simultaneously the height and the slope of the Gaussian part of the profile, and the slope in the deep region of the profile. The fit presented in Fig. 6 is the least accurate fit of our set.

The fit adjustments are very sensitive, and diffusion coefficients with three significant digits can be obtained. However, considering the experimental inaccuracies due to SIMS measurements, we preferred to adjust the diffusion coefficients with only two significant digits. The best fit is based on the overall profile and adjusted with two parameters D_g and D_{gb}. Nevertheless, several D_g-D_{gb} pairs corresponding to fits that are less accurate but acceptable considering the SIMS data can be found. These values are used to determine the measurement error of the coefficients D_g and D_{gb} independently. Typically, this error is between 10% and 20%. The Ge diffusion coefficients measured in the nanograins and in the nano-GBs are presented with their error bars in Fig. 7. The Arrhenius plots give $D_g^{Ge}=1.97\times10^{-4}\exp(-2.92$ eV$/kT)$ and $D_{gb}^{Ge}=1.68\times10^{4}\exp(-3.54$ eV$/kT)$ cm^2 s^{-1}.

Author complimentary copy. Redistribution subject to AIP license or copyright, see http://jap.aip.org/jap/copyright.jsp

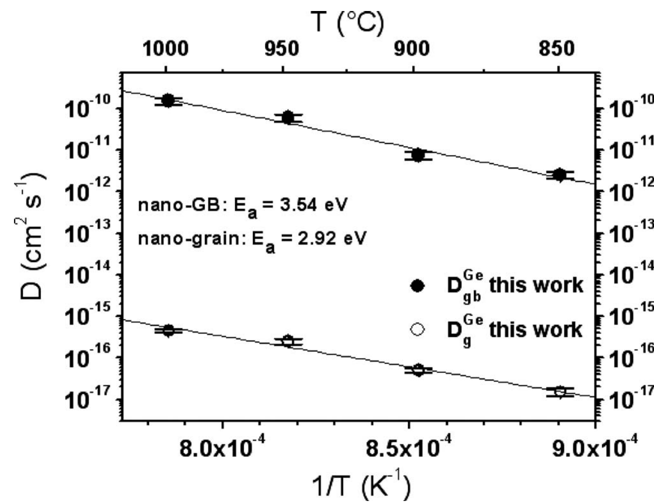

FIG. 7. Ge diffusion coefficients vs 1/T (K^{-1}) measured in the Si nanograins (D_g, ○) and in the nano-GBs (D_{gb}, ●) using the Fisher model solved via the finite element technique.

V. DISCUSSION

The diffusion coefficient in microscopic grains is known to be the same as that in Si bulk.[1–4] In Fig. 8, the diffusion coefficients measured in the 40 nm wide grains are compared with D_b measured by three different authors: Dorner *et al.*[22] ($D_b^{Ge}=1.03\times 10^5 \exp(-5.34\ \text{eV}/kT)\ \text{cm}^2\ \text{s}^{-1}$), Hettich *et al.*[23] ($D_b^{Ge}=0.35 \exp(-3.93\ \text{eV}/kT)\ \text{cm}^2\ \text{s}^{-1}$), and Zangenberg *et al.*[24] ($D_b^{Ge}=310 \exp(-4.65\ \text{eV}/kT)\ \text{cm}^2\ \text{s}^{-1}$). The in-grain diffusion coefficient in the nanocrystalline matrix is found to be at least one order of magnitude higher than in a microcrystalline matrix, and the activation energy of diffusion (E_a) is found to be at least 1 eV lower in the nanograins than in Si bulk. Simulations (not presented here) have shown that if the Ge diffusion coefficient in the mono-Si substrate was the same as in the Si nanograins, diffusion would have been clearly observed in the SIMS profiles in the mono-Si substrate (especially at 1000 °C). Enhanced diffusion in grains reported in literature has always been explained considering grain growth (i.e., GB migration).[4] Despite that the possible effect of GB migration cannot be completely excluded, no evidence of grain growth has been detected in our case; the grains have the same average size before and after annealing. Furthermore, as the poly-Si layer is directly deposited on the mono-Si substrate, GB migration is expected to favor Si homoepitaxy at the poly-Si /mono-Si interface, leading to the migration of this interface and thus to a reduction in thickness of the poly-Si layer. This has not been observed in any of our samples.

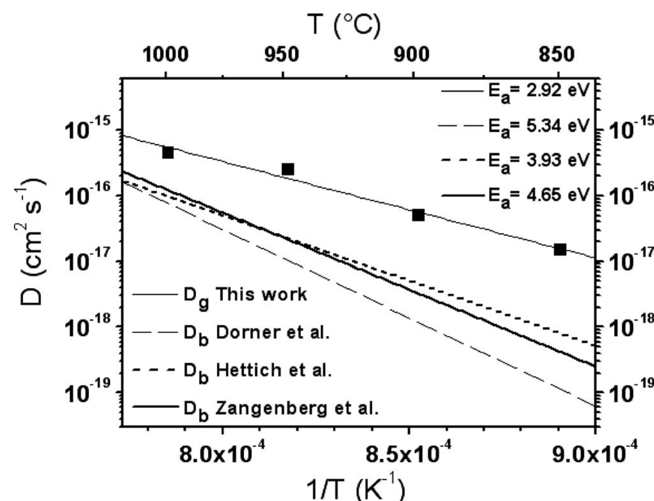

FIG. 8. Ge diffusion coefficient vs 1/T (K^{-1}) measured in the Si nanograins (D_g, ■) compared to the Ge diffusion coefficient in Si bulk measured by several authors: Dorner *et al.* (Ref. 22) (– –), Hettich *et al.* (Ref. 23) (- - -) and Zangenberg *et al.* (Ref. 24) (—).

Diffusion in nanoparticles has not been extensively studied, and only independent particles with sizes lower than 20 nm are (theoretically) expected to present enhanced diffusion,[26] due to the size dependence of vacancy formation energy in nanoparticles.[27] However, variable-energy positron annihilation experiments have shown that point defect concentrations are different in the vicinity of the surface from deep in the bulk.[28–30] In some cases, in order to find a constant vacancy concentration in the bulk of the crystal, a depth greater than 100 nm from the surface needs to be reached. Thus, grains having dimensions less than 100 nm can have point defect densities quite different from that in the bulk, and consequently a different diffusion coefficients. Ge diffusion in Si is considered to be vacancy mediated[23] for temperatures lower than 1000 °C and Si self-interstitials[23] mediated at higher temperatures. Our measurements were performed in a temperature range (850–1000 °C) corresponding to vacancy-mediated Ge diffusion. Consequently, the increase in the diffusion coefficient in the nanograins could be explained considering an increase in the vacancy concentration due to the influence of the nanograin surfaces. This interpretation is consistent with the decrease in the activation energy in the nanograin. We found E_a=2.92 eV, considering that the vacancy migration energy is about 0.45 eV in Si,[31] the vacancy formation energy in the nanograins would be ~2.47 eV. Despite the low activation energy measured in the nanograin, this value is still reasonable since measurements[32–34] and first principal calculations[35,36] give formation energy values between 2.1 and 3.8 eV for a monovacancy in Si.

In Fig. 9, the Ge diffusivity measured in the nano-GBs is compared to the diffusivity measured in microcrystalline GBs using Dorner *et al.*[22] and Hettich *et al.*[23] data for the Ge bulk diffusion in Si. The Ge diffusion in nano-GBs is found to be about one order of magnitude higher than in micro-GBs. However, the activation energy in nano- and micro-GBs is found to be almost the same; while the activation energy difference is ~1 eV in the bulk, it is only 0.2 eV in the GBs considering Hettich *et al.*[23] data. The activation energy found in the nano-GBs is closer to the value found in micro-GBs using the bulk diffusivity from Hettich *et al.*[23] than to the one obtained using Dorner *et al.*[22] data. This can be understood considering that the Arrhenius law given by Dorner *et al.*[22] was defined by considering diffusion coefficients measured over the entire temperature range from 850 to 1300 °C, without taking into consideration the diffusion mechanism change at about 1000 °C (from vacancy to self-interstitial mediated diffusion), whereas Hettich *et al.*[23] have given two Arrhenius laws, using two temperature ranges cor-

Author complimentary copy. Redistribution subject to AIP license or copyright, see http://jap.aip.org/jap/copyright.jsp

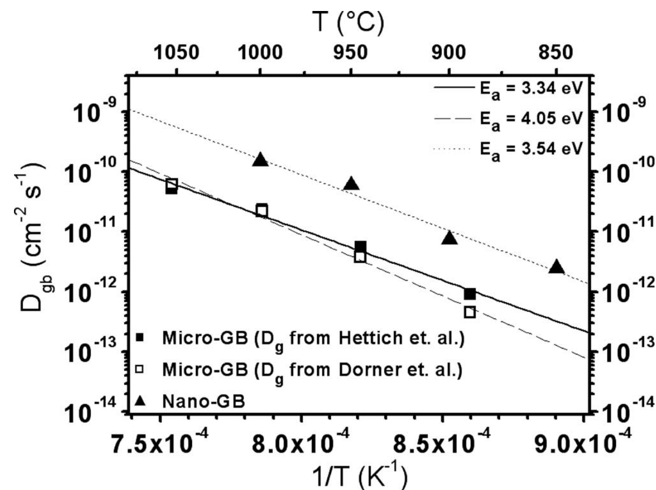

FIG. 9. Ge diffusion coefficients vs 1/T (K^{-1}) measured in the Si nano-GBs (D_{gb}, ▲), and in the Si micro-GBs using the Ge diffusion coefficient in Si bulk (D_b) measured by different authors: Dorner *et al.* (Ref. 22) (□) and Hettich *et al.* (Ref. 23) (■).

responding to the two different diffusion mechanisms. In Fig. 9 we used the Arrhenius law from Hettich *et al.*[23] corresponding specifically to the temperature range of our experiments (i.e., vacancy mediated mechanism).

In general, variations in the overall value of the GB diffusion coefficient can be due to a change in diffusion mechanism but also to different phenomena such as impurity interactions, impurity GB segregation, GB orientation etc., while the activation energy is more closely related to the diffusion mechanism. Consequently, the diffusion mechanism appears to be the same in nano- and micro-GBs. Technically, if the activation energies are similar, the difference between two diffusion coefficients is concentrated in the Arrhenius prefactor, which contains among several factors (such as geometry, correlation…) the entropic component. Due to experimental uncertainties and the difficulties to link the prefactor value to the structural and thermodynamic characteristics of the experimental GBs, it is usually risky to support too much interpretation on the prefactor. However, the global increase in the diffusivity in nano-GBs compared to the diffusivity in micro-GBs can be simply explained by considering impurity GB segregation. Even if the impurity (carbon, etc.) concentrations are below the detection limit (of SIMS for example) in the layers, a non-negligible concentration of these impurities can segregate in the GBs. For the same bulk impurity concentration, the concentration of segregated impurities in GBs should be lower in layers with higher GB density. The surface area available for impurity segregation is $\sim 10^3$ times greater in a layer made of 40 nm wide grains than in a layer made of 30 μm wide grains. The smaller the size of the grains is, the cleaner the GBs are. Since impurity GB segregation has been shown to decrease the mobility of diffusing species in GBs,[37] it is not surprising to observe a faster GB diffusivity in nanocrystalline layers compared to microcrystalline layers. Furthermore, since in our case the production of the microcrystalline layer and that of the nanocrystalline layer were different, their impurity content may also be different.

For microcrystalline layers of pure elements, we usually expect the bulk activation energy to be lower than the activation energy in GBs. However, in our case the activation energy in GBs is found to be $\sim$0.6 eV higher than in the grains. This can be explained considering that the nanosize effect is different in grains and in GBs. The decrease in the grain size leads to the modification of the bulk properties of the grains but not of the average properties of the GBs. This leads to an atypically low activation energy in the grains and to a standard activation energy in the GBs.

Finally, the effect of GB TJs needs to be discussed. The effect of TJs is expected to be negligible in our experiments, as layers made of 40 nm wide grains do not promote a high density of atomic site in TJs.[38] This is why we did not consider their influence in our interpretations. However, recent theoretical considerations[39] suggested that in our annealing temperature range $(0.55 \leq T/T_m \leq 0.75)$, the type *A* kinetic regime of diffusion may involve TJs in addition to GBs in fcc and bcc crystals, even for 50 nm grains. In this case, the Fisher model geometry would not accurately describe the diffusion in the polycrystalline layer. A 3D model depicting TJ diffusion in addition to grain and GB diffusion would therefore be needed.

VI. CONCLUSION

In conclusion, the Ge diffusivity in micro and nanocrystalline Si has been measured and compared using the well known Fisher model. In the nanocrystalline layer, both the diffusion coefficients in nanograins and in nano-GBs have been measured. Ge diffusion in Si nanograins is at least one order of magnitude faster than in mono-Si, and the activation energy of diffusion is at least 1 eV lower in the nanograins than in Si bulk. Ge diffusivity is also faster in nano-GBs than in conventional micro-GBs. However, the activation energy is nearly the same in nano-GBs and in micro-GBs. These observations were interpreted considering that the influence of TJs is negligible in these experiments, and that the nanosize effect increases the vacancy concentration in nanograins compared to bulk due to the influence of the grain surfaces, while it does not drastically change the nature of GBs. The authors would like to stress that the nanosize effect observed here in Si may be completely different than in polycrystalline metals since the nature and the density of point defects, as well as the kinetics to reach point-defect equilibrium in semiconductors, are different from metals.

[1] C. E. Allen, D. L. Beke, H. Bracht, C. M. Bruff, M. B. Dutt, G. Erdélyi, P. Gas, F. M. d'Heurle, G. E. Murch, E. G. Seebauer, B. L. Sharma, and N. A. Stolwijk, *Diffusion in Semiconductors and Non-Metallic Solids*, Landolt-Börnstein-Numerical Data and Functional Relationships in Science and Technology, edited by D. Beke (Springer-Verlag, Berlin, 1998), Vol. 33, Pt. A.
[2] J. C. Fisher, J. Appl. Phys. **22**, 74 (1951).
[3] I. Kaur, Y. Mishin, and W. Gust, *Fundamentals of Grain and Interphase Boundary Diffusion* (Wiley, Chichester, 1995).
[4] Y. Mishin, C. Herzig, J. Bernardini, and W. Gust, Int. Mater. Rev. **42**, 155 (1997).
[5] M. Koppers, Y. Mishin, and C. Herzig, Acta Metall. Mater. **42**, 2859 (1994).
[6] J. Bernardini, C. Girardeaux, and A. Rolland, Interface Sci. **11**, 33 (2003).
[7] S. G. Srinivasan, J. W. Cahn, H. Jónsson, and G. Kalonji, Acta Mater. **47**, 2821 (1999).

Author complimentary copy. Redistribution subject to AIP license or copyright, see http://jap.aip.org/jap/copyright.jsp

[8] I. A. Ovid'ko and A. G. Sheinerman, Rev. Adv. Mater. Sci. **6**, 41 (2004).
[9] *Nanodiffusion—Diffusion in Nanostructured Materials*, Special Issue J. Metastable Nanocryst. Mater., edited by D. L. Beke (Trans Tech Publications, 2004), Vol. 19.
[10] D. L. Beke and Z. Erdélyi, Phys. Rev. B **73**, 035426 (2006).
[11] Y. Chen and C. A. Schuh, Acta Mater. **54**, 4709 (2006).
[12] J. Bernardini, C. Girardeaux, Z. Erdelyi, and C. Lexcellent, J. Metastable Nanocryst. Mater. **19**, 35 (2004).
[13] W. P. Tong, N. R. Tao, Z. B. Wang, J. Lu, and K. Lu, Science **299**, 686 (2003).
[14] Z. Erdelyi, M. Sladecek, L. M. Stadler, I. Zizak, G. A. Langer, M. K. Varga, D. Beke, and B. Sepiol, Science **306**, 1913 (2004).
[15] Z. Balogh, Z. Erdélyi, D. L. Beke, G. A. Langer, A. Csik, H.-G. Boyen, U. Wiedwald, P. Ziemann, A. Portavoce, and C. Girardeaux, Appl. Phys. Lett. **92**, 143104 (2008).
[16] B. Bokstein, V. Ivanov, O. Oreshina, A. Peteline, and S. Peteline, Mater. Sci. Eng., A **302**, 151 (2001).
[17] T. Suzuoka, Trans. Jpn. Inst. Met. **2**, 25 (1961).
[18] www.comsol.com for precise description of this software.
[19] T. Suzuoka, J. Phys. Soc. Jpn. **19**, 839 (1964).
[20] S. Solmi, M. Ferri, M. Bersani, D. Giubertoni, and V. Soncini, J. Appl. Phys. **94**, 4950 (2003).
[21] M. Petravić, B. G. Svensson, and J. S. Williams, Appl. Phys. Lett. **62**, 278 (1993).
[22] P. Dorner, W. Gust, B. Predel, U. Roll, A. Lodding, and H. Odelius, Philos. Mag. A **49**, 557 (1984).
[23] G. Hettich, H. Mehrer, and K. Maier, Inst. Phys. Conf. Ser. **46**, 500 (1979).
[24] N. R. Zangenberg, J. Lundsgaard Hansen, J. Fage-Pedersen, and A. Nylandsted Larsen, Phys. Rev. Lett. **87**, 125901 (2001).
[25] G. L. McVay and A. R. Ducharme, Phys. Rev. B **9**, 627 (1974).
[26] K. Dick, T. Dhanasekaran, Z. Zhang, and D. Miesel, J. Am. Chem. Soc. **124**, 2312 (2002).
[27] W. H. Qi and M. P. Wang, Physica B (Amsterdam) **334**, 432 (2003).
[28] Z. L. Peng, P. J. Simpson, and P. Mascher, Electrochem. Solid-State Lett. **3**, 150 (2000).
[29] M. Fujinami, T. Miyagoe, T. Sawada, and T. Akahane, J. Appl. Phys. **94**, 4382 (2003).
[30] J. Oila, J. Kivioja, V. Ranki, K. Saarinen, D. C. Look, R. J. Molnar, S. S. Park, S. K. Lee, and J. Y. Han, Appl. Phys. Lett. **82**, 3433 (2003).
[31] G. D. Watkins, Mater. Sci. Semicond. Process. **3**, 227 (2000).
[32] H. Bracht, J. Fage Pedersen, N. Zangenberg, A. Nylandsted Larsen, E. E. Haller, G. Lulli, and M. Posselt, Phys. Rev. Lett. **91**, 245502 (2003).
[33] J. A. Van Vechten, Phys. Rev. B **33**, 2674 (1986).
[34] S. Dannefaer, P. Mascher, and D. Kerr, Phys. Rev. Lett. **56**, 2195 (1986).
[35] F. El-Mellouhi, N. Mousseau, and P. Ordejón, Phys. Rev. B **70**, 205202 (2004).
[36] D. Caliste, P. Pochet, T. Deutsch, and F. Lançon, Phys. Rev. B **75**, 125203 (2007).
[37] B. Semmache, A. Merabet, C. Gontrand, and A. Laugier, Mater. Sci. Eng., B **38**, 41 (1996).
[38] M. A. Fortes, Mater. Sci. Forum **126–128**, 343 (1993).
[39] Y. Chen and C. A. Schuh, J. Appl. Phys. **101**, 063524 (2007).

Author complimentary copy. Redistribution subject to AIP license or copyright, see http://jap.aip.org/jap/copyright.jsp